Computer-simulation study of the interface between graphite and hydrocarbon mixtures: Preferential adsorption and dynamics

M. J. Kotelyanskii* and R. Hentschke

Max-Planck-Institut für Polymerforschung, Ackermannweg 10, 55128 Mainz, Germany

We study the competitive adsorption from two different mixtures containing benzene and n-heptane onto graphite using constant-temperature molecular-dynamics simulations at 300 K. While the preferential adsorption of either benzene or n-heptane is observed for the two different compositions, the graphite surface is always covered by a dense liquidlike monolayer formed by the n-heptane chains, lying parallel to the surface. We also investigate the molecular structure and mobility in the vicinity of the surface in comparison to the bulk solution.

Modification of interfacial properties through adsorption from solution plays an important role in the context of corrosion, lubrication, adhesion, wetting, colloidal stability, flocculation, or molecular recognition [1–3]. Even though experimental methods such as the measurement of the amount adsorbed, calorimetric studies, infrared spectroscopy, ellipsometry, neutron scattering [1,2], or the surface force apparatus [4] allow one to study the solid-solution interface, the extraction of structural and dynamical information on the molecular scale is not always possible. An exception is the crystalline monolayers formed, for instance, by alkyl derivatives adsorbing from organic solutions onto graphite (and other substrates), which can be imaged with molecular resolution under *in situ* conditions using scanning-tunneling [5] or scanning-force microscopy [6]. Analytical models of adsorption from a solution are usually based on either lattice descriptions of both surface and solution or on assuming homogeneous structureless surfaces in equilibrium with likewise structureless liquids (e.g., [2,7]), and thus are often difficult to apply to a specific system. It is this which makes the atomistic modeling of the solid-solution interface an interesting application and testing ground for computer-simulation techniques.

Here we apply the molecular-dynamics method to liquid hydrocarbon mixtures confined to a narrow slit between graphite basal planes. The solution molecules are placed into a computational cell with periodic boundary conditions parallel to the surfaces. We consider two mixtures, consisting of 72 benzene and 400 heptane molecules (benzene mole fraction $x_0^b = 0.18$) and 216 benzene and 240 heptane molecules (benzene mole fraction $x_0^b = 0.474$), respectively.

Intermolecular and intramolecular interactions within the solution are calculated according to the AMBER force field [8], while the solid-solution interactions are described via an external field based on the summation of atom-atom Lennard-Jones (LJ) interactions [cf. Eqs. (1)–(3) in Ref. [9] for the full potential function]. We use the all-atom representation for the benzene molecules, in order to reproduce the proper partial charge distribution on the benzene ring. The interbenzene and intrabenzene as well as the solid-benzene potential parameters are the same as in Table I of [9]. For the CH_2 and CH_3 groups along the heptane chain we use the united-atom or pseudoatom representation, neglecting the charges [9]. The interheptane and intraheptane parameters are again taken from the AMBER database (cf. Table I). LJ cross parameters between benzene and heptane are calculated using the Lorentz-Berthelot mixing rules. The LJ parameters for interactions of pseudoatoms with the solid (cf. Table I) are obtained by fitting the adsorption potential of the pseudoatom heptane chain (treating CH_2 and CH_3 groups as identical) to the adsorption potential of the all-atom heptane chain, based on the parameters in Table I of [9]. During the simulation, all nonbonded intrasolution interactions beyond a residue-based cutoff of 8 Å are omitted.

Keeping the bond lengths constant via the SHAKE algorithm [10], we integrate the equations of motion using the leap-frog Verlet algorithm [11] with a time step of 1.5 fs. We fix the cell dimensions parallel to the surface at 43.6 Å × 43.6 Å for both mixtures. The intersurface spacing is adjusted to yield the bulk density in the middle of the cell, which yields intersurface separation of 59.00 Å for $x_0^b = 0.18$ and 48.289 Å for $x_0^b = 0.474$. The bulk densities $\rho_{bulk} = 0.70$ g/cm³ for $x_0^b = 0.18$ and $\rho_{bulk} = 0.75$ g/cm³ for $x_0^b = 0.474$ we obtain from the experimental densities of the pure components using the volume additivity rule, which here is applicable to within 0.1% [12]. During each of the two 3-ns simulation runs a constant temperature of 300 K is maintained using velocity scaling [13]. The final 1.5 ns of each run is included in the analysis.

Figure 1 shows the molecular center-of-mass distribution and the benzene mole fraction profiles perpendicular to the surfaces. (a) and (b) show that for both compositions the graphite surface is covered by a dense layer (cf. the peaks at ∼4 Å) of flatly adsorbed heptane molecules.

---

*Permanent address: Institute of Chemical Physics of the Russian Academy of Sciences, ul. Kosygina, 4 Moscow, Russia.

TABLE I. Parameters describing the intramolecular and intermolecular interactions of the n-heptane molecules. Here r_{eq} is the bond length. Note also that the valence angle potential is $U_{ang} = f_\delta(\delta - \delta_{eq})^2$, the dihedral angle potential is $U_{dih} = f_n\{1 + \cos(n\phi - \gamma)\}$, and the LJ potential is $U_{LJ} = \varepsilon\{(\sigma/r)^{12} - 2(\sigma/r)^6\}$, where $\sigma = \sigma_i + \sigma_j$, and $\varepsilon = \sqrt{\varepsilon_i \varepsilon_j}$ (cf. [9]).

Bonds		r_{eq} (Å)	
CH_2—CH_2		1.53	
CH_2—CH_3		1.53	
Angles	f_δ (kcal mol^{-1})	δ_{eq} (deg)	
CH_2—CH_2—CH_2	63.0	112.4	
CH_2—CH_2—CH_3	63.0	112.4	
Dihedrals	f_n (kcal mol^{-1})	γ	n
x—CH_2—CH_2—x	2.0	0.0	3
LJ parameters	ε_i (kcal mol^{-1})	σ_i (Å)	
CH_2	0.12	1.925	
CH_3	0.15	2.000	
n-heptane–graphite LJ parameters	ε (kcal mol^{-1})	σ (Å)	
CH_2—G	0.797	4.19	
CH_3—G	0.797	4.19	

The area per heptane chain in this layer is equal to (52.0 ± 2.5) Å^2 for $x_0^b = 0.18$, and (51.6 ± 2.5) Å^2 for $x_0^b = 0.474$. A similar segregation was also obtained in a recent simulation of an n-alkane mixture on Au(001) [14].
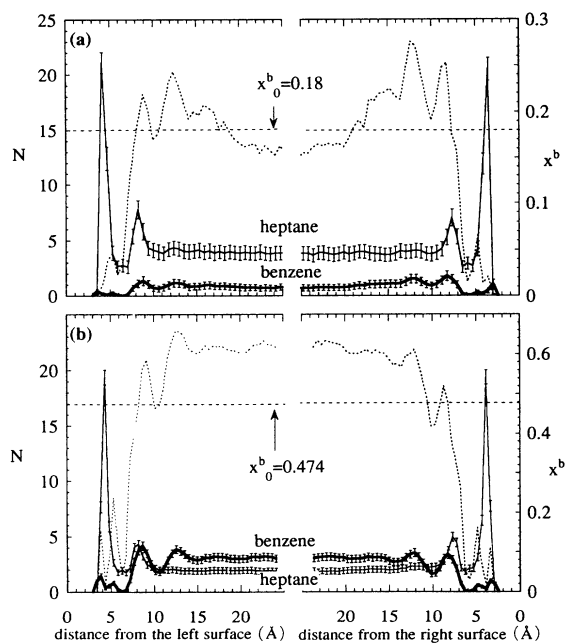

FIG. 1. Center-of-mass frequency N (left axis, solid lines) of the heptane (thin lines) and benzene (thick lines) molecules, and benzene mole fraction x^b (right axis, dotted lines) as functions of the distance from the graphite surfaces. Error bars represent the mean-squared deviations. (a), $x_0^b = 0.18$. (b), $x_0^b = 0.474$. Here, x_0^b, indicated by the horizontal dashed lines, is the benzene bulk mole fraction in the absence of the surfaces.

Notice that the occupation of this first layer does not significantly reflect the strongly different compositions of the bulk phase. In the second layer (cf. the peaks at 8.5 Å) the heptane concentration decreases significantly, whereas in both cases the layer is enriched by benzene molecules. For both compositions the surface-induced solvation shell structure extends out to about 15 Å. However, the heptane profile is essentially featureless beyond the second layer.

The effect of the surface on the local composition is better illustrated by the benzene mole fraction profiles x^b. Notice that for the case where the average benzene mole fraction is $x_0^b = 0.18$, Fig. 1(a) shows a pronounced surface enrichment of benzene between 8 and 18 Å from the surface, where $x^b > x_0^b$. In contrast, for $x_0^b = 0.474$, as shown in Fig. 1(b), the overall effect of the surfaces on x^b is more monotone and, in particular, $x^b > x_0^b$ for large distances from the surface.

Experimental comparisons of the bulk value of x^α where α is component of interest in a binary mixture, with x_0^α are often used to indirectly infer whether or not the component α is preferentially adsorbed at a specific solid-liquid interface. More precisely, if $x^\alpha < x_0^\alpha$ in the bulk, the species α is considered to be preferentially adsorbed.

Notice, however, that this only allows us to determine an average preferential enrichment of α across the width of the interface. It does not signify that α is in direct contact with the solid. Figure 1(a), i.e., $x_0^b = 0.18$, illustrates this point. Here, $x^b < x_0^b$ in the bulklike region near the center of the slit, which would indicate the preferential adsorption of benzene on graphite for this value of x_0^b (in qualitative agreement with experimental observations [15]). However, the simulation shows that the

layer closest to the surface is predominantly occupied by heptane.

To characterize the structure within the adsorbed heptane layer, i.e., the layer closest to the surface, we calculate the in-plane heptane center-of-mass pair-correlation function $g_2(R)$, which is shown in Fig. 2(a). Here, R is the projection of the center-of-mass distance onto the surface plane. Notice that the short-range order ($R < 8$ Å) in the adsorbed layer is more pronounced in comparison to the bulklike region near the center of the slit where we observed no distinct first peak. Notice also that the short-range order is weaker for $x_0^b = 0.18$ in comparison to $x_0^b = 0.474$.

The orientational ordering of the heptane molecules in the first layer is described by the in-plane orientation pair-correlation function $G(R)$, which measures the in-plane alignment of the chains with respect to each other as a function of their in-plane center-of-mass separation R. Here, $G(R)$ is defined as $G(R) = \langle \cos^2 \phi_{ij} \rangle_R$, where ϕ_{ij} is the angle between the projections of the end-to-end vectors of chains i and j onto the plane parallel to the surface. The brackets $\langle \ \rangle_R$ stand for the average over all pairs of chains, whose in-plane center-of-mass separation is R. Figure 2(b) shows that $G(R)$ virtually coincides for the two mixtures. Independent of composition there is a significant alignment of neighboring chains. The overall orientation correlations extend out to $R \sim 15$ Å, which is the distance between second nearest neighbors. This is

different near the center of the slit, where only weak correlations between the orientations of adjacent chains (out to $R \sim 8$ Å) are observed.

Figure 3 shows that the surface heptane layers exhibit pronounced liquidlike translational [panel (a)] and orientational [panel (b)] mobility. Nevertheless, in both mixtures, both the translation and orientation diffusion coefficients are significantly lower than in the bulk solution (due to the change in dimensionality and, in addition, possibly due to the cooperativity suggested by the strong orientation correlation between adjacent chains). The translation self-diffusion coefficients (defined by $D_t = \lim_{t \to \infty} (d \langle \Delta r_{xy}^2 \rangle)/dt /4$, where $\langle \Delta r_{xy}^2 \rangle$ is the mean square projection of the displacement vector onto the graphite plane, and t is the time) for the heptane chains in the surface layer are 0.43 Å²/ps for $x_0^b = 0.18$ and 0.32 Å²/ps for $x_0^b = 0.474$, whereas the corresponding values
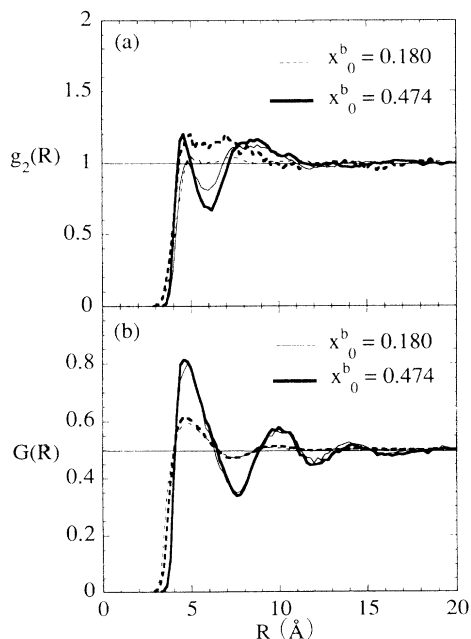

FIG. 2. (a) In-plane heptane center-of-mass pair-correlation function $g_2(R)$, where R is the projection of the distance between the centers of mass of two heptane molecules onto the surface plane. The solid lines are for molecules within the first adsorbed layer less than 5 Å from the surfaces, whereas the dashed lines are for molecules within a 5-Å slab along the center of the slit. The thin lines correspond to $x_0^b = 0.18$, and the thick lines to $x_0^b = 0.474$. (b) Same as (a) but for the corresponding orientation pair-correlation function $G(R)$.
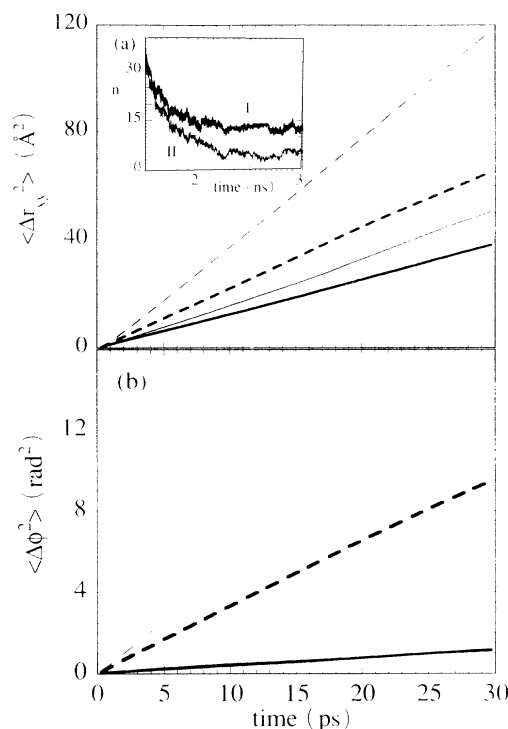

FIG. 3. (a) Translational diffusion. The mean-square projection of the center-of-mass displacement of the heptane molecules onto the graphite plane $\langle \Delta r_{xy}^2 \rangle$ vs time. The solid lines include all molecules within the first adsorbed layer less than 5 Å from the surfaces, whereas the dashed lines include all molecules above 15 Å from the surface. The thin lines correspond to $x_0^b = 0.18$ and the thick lines correspond to $x_0^b = 0.474$. The inset illustrates the time scale of the bulk-surface equilibration. Line I corresponds to $x_0^b = 0.18$ and line II corresponds to $x_0^b = 0.474$. Here, n is the number of heptane molecules adsorbed at a surface (i.e., center-of-mass distance from the surface < 5 Å) at time t under the condition that the same molecules were adsorbed at the same surface at $t = 1.5$ ns. (b) Orientational diffusion. Mean-squared deviation of the angle ϕ between the projection of the heptane end-to-end vector onto the surface plane and a fixed axis in the same plane vs time. The line types correspond to (a). Note that the thin solid line is covered by the thick solid line.

for the bulk solutions are 1.00 and 0.55 Å^2/ps. Here, bulk refers to the heptane chains whose center-of-mass separation from the surfaces is larger than 15 Å. The corresponding surface orientation self-diffusion coefficients [defined by $D_\phi = \lim_{t \to \infty} (d \langle \Delta\phi^2 \rangle /dt)/2$] are 0.019 rad^2/ps for $x_0^b = 0.18$ and 0.017 rad^2/ps for $x_0^b = 0.474$, whereas the corresponding values in the bulk solution are 0.51 rad^2/ps and 0.31 rad^2/ps.

Notice also in this context that the surface heptane layer and the bulk solution are in dynamic equilibrium [cf. the inset in Fig. 3(a)], i.e., while the number of the molecules adsorbed on the graphite surface do not vary with time, and there is a permanent exchange between the surface layer and the bulk solution. After 200 ps about 50% of the chains initially adsorbed in the first layer are replaced by chains from the outer part of the interface or from the bulk solution. Thus, in addition to lateral mobility there is also a considerable normal mobility of the heptane molecules in the interface, which should preclude the imaging of such layers of short n-alkanes using tip microscopies (at room temperature). Indeed, images of corresponding (lamellar) ordered n-alkane monolayers on graphite at room temperature have so far only been obtained for $C_{16}H_{34}$ and longer chains [16].

[1] *Adsorption from Solution,* edited by R. H. Ottewill, C. H. Rochester, and A. L. Smith (Academic, London, 1983).

[2] *Adsorption from Solution at the Solid/Liquid Interface,* edited by G. D. Parfitt and C. H. Rochester (Academic, London, 1983).

[3] *Surfactants,* edited by Th. F. Tadros (Academic, London, 1984).

[4] J. N. Israelachvili, *Intermolecular and Surface Forces* (Academic, London, 1985).

[5] J. P. Rabe and S. Buchholz, Science **253**, 424 (1991); Phys. Rev. Lett. **66**, 2096 (1991).

[6] L. M. Eng, H. Fuchs, S. Buchholz, and J. P. Rabe, Ultramicrosc. **42-44**, 1059 (1992).

[7] R. Dickman, J.-S. Wang, and I. Jensen, J. Chem. Phys. **94**, 8252 (1991).

[8] S. J. Weiner, P. A. Kollman, D. A. Case, U. C. Singh, C. Ghio, G. Alagona, S. Profeta, and P. Weiner, J. Am. Chem. Soc. **106**, 765 (1984).

[9] R. Hentschke and R. G. Winkler, J. Chem. Phys. **99**, 5528 (1993).

[10] W. F. van Gunsteren and H. J. C. Berendsen, Mol. Phys. **34**, 1311 (1977).

[11] M. P. Allen and D. J. Tildesley, *Computer Simulations of Liquids* (Clarendon, Oxford, 1990).

[12] A. M. Awwad, S. F. Al-Azzawi, and M. A. Salman, Fluid Phase Equilibria **31**, 171 (1986).

[13] H. J. C. Berendsen, J. P. M. Postma, W. F. van Gunsteren, A. DiNola, and J. R. Haak, J. Chem. Phys. **81**, 3684 (1984).

[14] T. K. Xia and U. Landmann, Science **261**, 1310 (1993).

[15] S. G. Ash, R. Brown, D. H. Everett, J. Chem. Thermodynamics **5**, 239 (1973); J. Chem. Soc. Faraday Trans. **71**, 123 (1975).

[16] J. P. Rabe (private communication).